Characterization of γ-$Ga_2O_3-Al_2O_3$ Prepared by Solvothermal Method and Its Performance for Methane-SCR of NO

Tetsu Nakatani,[†] Tsunenori Watanabe,[†,‡] Masaru Takahashi,[†] Yuya Miyahara,[†] Hiroshi Deguchi,[‡] Shinji Iwamoto,[†] Hiroyoshi Kanai,[†] and Masashi Inoue*[,†]

Department of Energy and Hydrocarbon Chemistry, Graduate School of Engineering, Kyoto University, Katsura, Kyoto 615-8510, Japan, and Power Engineering R&D Center, The Kansai Electric Power Company, Inc., 3-11-20, Nakoji, Amagasaki 661-0974, Japan

Received: February 20, 2009; Revised Manuscript Received: April 26, 2009

The γ-$Ga_2O_3-Al_2O_3$ mixed oxides with a spinel structure were prepared by the solvothermal reaction of gallium acetylacetonate and aluminum isopropoxide in diethylenetriamine. In the crystal structures of the catalysts obtained by the calcination of these mixed oxides, Ga^{3+} and Al^{3+} ions preferentially occupied tetrahedral and octahedral sites, respectively. The catalysts with low Ga contents had a unique structure with high surface areas and a concentration gradient of decreasing Ga content from the surface to the bulk. In methane-selective catalytic reduction (SCR) of NO, higher NO conversion to N_2 was attained on the catalyst with high occupation of Ga^{3+} ions at tetrahedral sites and Al^{3+} ions at octahedral sites. For the γ-$Ga_2O_3-Al_2O_3$ mixed oxide with a charged Ga molar content of 0.3 (ST(0.3)), tetrahedral and octahedral sites were solely occupied by Ga^{3+} and Al^{3+} ions, respectively, and the catalyst exhibited the highest NO conversion to N_2. Therefore, it was concluded that the active site for methane-SCR of NO is tetrahedral Ga^{3+} ion and octahedral Al^{3+} ion, which are linked to each other. Nitrogen monoxide is adsorbed on the isolated hydroxyl group attached to Al^{3+} ions and then oxidized by O_2 yielding surface nitrate species. Tetrahedral Ga^{3+} ions work as Lewis acid sites for the activation of methane because of their coordinative unsaturation. The Ga^{3+} ions in the γ-$Ga_2O_3-Al_2O_3$ catalyst have a redox property, which plays important roles in both the oxidation of NO to surface nitrate species and the activation of methane. The most important factor for this catalyst is that the sites for the formation of surface nitrate species reside next to the methane activation sites, which facilitates the reaction between surface nitrate species and the activated species derived from methane, thus mitigating the consumption of methane by simple combustion with O_2. Therefore, ST(0.3), which has the largest number of ensembles of the tetrahedral Ga^{3+} ions and octahedral Al^{3+} ions, shows the highest activity for methane-SCR of NO.

1. Introduction

Among the various strategies for removing NO_x from exhaust gases, selective catalytic reduction (SCR) using methane as a reductant[1−5] is an attractive process because methane is the main component of natural gas, an abundant resource that is used as a fuel for power stations. Moreover, methane can be easily removed by catalytic combustion even if methane leaks from the SCR devices.

Although various zeolite catalysts have high activities for methane-SCR of NO_x, they have poor hydrothermal stabilities; their frameworks are destroyed by exposure to high-temperature steam. Therefore, the development of active oxide-type catalysts with higher hydrothermal stabilities is necessary because the water content in the exhaust gases from stationary combustion plants is rather high.

Gallium oxide is an effective catalyst for dehydrogenation of paraffin to olefin,[6] and Ga-containing zeolites are active for NO_x removal using hydrocarbons as reducing agents.[7] Shimizu et al. reported that γ-alumina-supported gallium oxide (Ga_2O_3/γ-Al_2O_3) catalyst prepared by an impregnation method showed a high activity for SCR of NO_x with methane.[2,3] Haneda et al. reported that $Ga_2O_3-Al_2O_3$ prepared by a sol−gel method has high performance for SCR of NO_x with propene.[4]

Although various aqueous medium-based methods for synthesizing metal oxides such as sol−gel, coprecipitation, and hydrothermal methods have been studied, the synthesis of metal oxide using organic solvents has not been widely explored. Our laboratory has been exploring solvothermal synthesis of metal oxides in organic media,[8] where solvothermal reaction means the reaction in liquid media at high temperatures. Previously, we reported that the γ-$Ga_2O_3-Al_2O_3$ solid solution catalysts prepared by solvothermal methods showed higher activities than the impregnation catalysts for methane-SCR of NO.[9−12] The activities of the catalysts prepared by using various media were examined, and it was found that the catalyst activity increased with the increase in the crystallite size. Diethylenetriamine was found to be the best solvent for the solvothermal synthesis of the γ-$Ga_2O_3-Al_2O_3$ catalyst having high activities under both dry and wet conditions.[12] The influence of reducing agents (C1−C3 hydrocarbons) upon the SCR of NO on γ-$Ga_2O_3-Al_2O_3$ catalyst was investigated, and methane was found to be the least reactive reductant of the hydrocarbons examined.[13] Under wet conditions, NO conversion on the catalyst decreased for all hydrocarbons. The reactivity of paraffins, especially methane, was severely affected by the presence of water in the

* To whom correspondence should be addressed. Tel: +81 75 383 2478. Fax: +81 75 383 2479. E-mail: inoue@scl.kyoto-u.ac.jp.
† Kyoto University.
‡ The Kansai Electric Power Company.

10.1021/jp901569s CCC: $40.75
Published on Web 05/29/2009

feed. This result was explained by preferential adsorption of water to the adsorption sites for hydrocarbons.[13]

The mechanisms of NO reduction by hydrocarbon over gallia−alumina catalysts have been discussed by several researchers. Shimizu et al. examined the methane-SCR activity of Ga_2O_3/Al_2O_3 prepared by an impregnation method and concluded that Ga cations in the surface tetrahedral sites are the origin of the high performance of their catalyst.[3] They also proposed reaction mechanisms for hydrocarbon-SCR on Al_2O_3-based catalysts.[14] By using IR spectroscopy, He et al. investigated the reaction pathway of propane-SCR of NO over Ga_2O_3/Al_2O_3 prepared by an impregnation method.[15] They concluded that the propane-SCR of NO starts with partial oxidation of propane mainly by O_2 to surface carboxylates such as acetate and formate, which are highly reactive toward adsorbed NO (or NO-derived species) yielding nitrogen-containing organic surface species (e.g., isocyanides and cyanides). The coupling of nitrogen atoms to form N_2 was suggested to occur via the disproportionation reaction between such nitrogen-containing species and NO. They also concluded that the rate-determining step of the whole reaction cycle is the partial oxidation of propane.[15]

By using GC-MS and IR spectroscopy, Haneda et al. investigated the mechanism of propane-SCR of NO over $Ga_2O_3-Al_2O_3$ prepared by a sol−gel method.[16,17] They suggested that the reaction is initiated by the formation of adsorbed nitrate species via NO oxidation by O_2. The reaction between adsorbed nitrate species and C_3H_6 causes the formation of the allyl species, which reacts with NO_x yielding organic nitro compounds such as CH_3NO_2, $C_2H_3NO_2$, and $C_3H_7NO_2$. Hydrolysis of these nitro compounds is assumed to form nitriles (e.g., CH_3CN and $CH_2{=}CH{-}CN$), isocyanates (−NCO), and oxygenates. Further hydrolysis of isocyanates (or nitriles) yields organic amines and CO_2 (or carboxylic acid and NH_3), which react with NO_x to form N_2, as is well known for NH_3−SCR. Haneda et al. proposed that the formation of nitriles and isocyanates is effectively promoted by Ga_2O_3.[16,17]

We found that surface allyl species are formed upon the exposure of propylene to both tetrahedral and octahedral Ga sites of $Ga_2O_3-Al_2O_3$ catalyst, and the amount of allyl species adsorbed on the tetrahedral Ga sites correlates with the activity of the catalyst.[18] However, methane is much less reactive than C3 hydrocarbons,[13] and surface allyl species were not formed from methane.[18] Moreover, surface formate species, a possible intermediate for methane-SCR, is reported to be less stable than surface acetate species.[19]

Therefore, the reaction mechanisms for the methane-SCR of NO may be different from propane- or propene-SCR. In this work, methane-SCR of NO was carried out on the γ-$Ga_2O_3-Al_2O_3$ catalysts prepared by the solvothermal method using diethylenetriamine as a solvent. The factors controlling the catalytic activity were explored, and the reaction mechanisms will be discussed focusing on the individual roles of the Ga^{3+} and Al^{3+} ions.

2. Experimental Section

2.1. Preparation of the Catalysts. The catalysts were prepared by the solvothermal method developed in our laboratory.[8] Gallium triacetylacetonate ($Ga(acac)_3$; Mitsuwa Chemical) and aluminum triisopropoxide (AIP; Nacalai Tesque) with various Ga/Al ratios were suspended in 80 mL of diethylenetriamine (dEtA; Nacalai Tesque) in a test tube, and the tube was placed in a 200 mL autoclave. In the gap between the autoclave wall and the test tube, an additional 30 mL of dEtA was placed. After the air in the autoclave was purged with nitrogen, the autoclave was heated to 300 °C at a rate of 2.5 °C·min^{-1}, kept at 300 °C for 2 h, and then cooled to room temperature. The products were washed with acetone by vigorous mixing and centrifuging, air dried, and calcined at 700 °C for 30 min to remove the remaining organic impurities. The yields of the catalysts were over 95%. In this article, the catalyst is designated as ST(x), where x stands for the Ga/(Ga + Al) ratio in the feed composition for the solvothermal treatment.

2.2. Activity Test for the Catalysts. Catalyst tests for the SCR of NO with methane were carried out in a fixed-bed flow reactor. The catalysts were tabletted, pulverized into 10−22 mesh size, and placed into the reactor. The catalyst bed was heated to 650 °C in a helium flow and held at that temperature for 30 min. Then, the reaction gas composed of 1000 ppm NO, 2000 ppm CH_4, 6.7% O_2, and 2.5% H_2O with helium balance was introduced to the catalyst bed at $W/F = 0.3$ g·s·mL^{-1} (SV = ∼11 000 h^{-1}). The reaction temperature was decreased from 650 to 450 °C at 5 °C·min^{-1} and kept for 15 min at every 50 °C interval to attain the stationary state. The effluent gases from the reactor were analyzed with an online gas chromatograph (GL Science Micro GC CP-2002) equipped with a 4 m Molsieve 5A column (80 °C) and a 10 m Poraplot Q column (40 °C). NO conversion was calculated, as shown in eq 1

$$\text{NO conversion (\%)} = (2[N_2]/[NO])100 \qquad (1)$$

where $[N_2]$ is the concentration of N_2 in the effluent and [NO] is the concentration of NO in the fed gas. Note, however, that no NO_x species other than NO were detected during methane-SCR, as analyzed with a Pfeiffer Vacuum Omnistar GSD 301 O 1 quadrupole mass spectrometer (Q-Mass).

2.3. Characterization of the Catalysts. Powder X-ray diffraction (XRD) patterns were measured on a Shimadzu XD-D1 diffractometer using 30 kV, 900 W Cu Kα radiation and a carbon monochromator. Crystallite size was calculated from the half-height width of the (440) diffraction peak of the spinel structure using the Scherrer equation.

The BET surface area was calculated by the single-point method, and the samples were dried in a 30% N_2/He flow at 300 °C for 30 min prior to measurement.

The bulk Ga/Al ratios were analyzed with a Shimadzu ICPS-1000IV inductively coupled plasma atomic emission spectrometer (ICP-AES). The catalysts were dissolved in phosphoric acid at 80 °C and then diluted to about 0.2 g·L^{-1} with water. The surface Ga/Al ratios were determined with an ULVAC-PHI 5500 X-ray photoelectron spectrometer (XPS) with a hemispherical energy analyzer. Samples were mounted on indium foil and then transferred to an XPS analyzer chamber. The residual gas pressure in the chamber during data acquisition was less than 1×10^{-8} Torr (1 Torr = 133.3 N·m^{-2}). The spectra were measured at room temperature using Mg Kα radiation (15 kV, 400 W). The electron takeoff angle was set at 45°. Binding energies were referenced to the calibrated on the basis of C 1s of residual carbon at 284.6 eV.[20] Sputtering was performed by an Xe^+ ion beam generated at 3.0 kV.

X-ray absorption fine structure (XAFS) at the Ga K-edge was measured by a transmission mode at room temperature using the SPring-8 BL16B2 beamline. The X-ray was monochromatized by a Si(111) monochromator. The data were analyzed using the software "Athena and Artemis".[21] As standard samples, $ZnGa_2O_4$ in which Ga ions occupy octahedral sites and ST(0.1) in which Ga ions preferentially occupy tetrahedral sites were

TABLE 1: Surface Areas and Compositions of Ga_2O_3−Al_2O_3 Catalysts

		Ga/(Ga+Al) ratio				
			sputter time			
catalyst	surface area ($m^2 \cdot g^{-1}$)	bulk	0 min	1 min	3 min	5 min
ST(0.0)	212					
ST(0.1)	179	0.077				
ST(0.25)	177	0.218	0.244			
ST(0.3)	154	0.254	0.27	0.265	0.252	0.239
ST(0.375)	131		0.379			
ST(0.5)	162	0.511	0.509	0.499	0.501	0.512
ST(0.75)	133	0.773	0.775	0.783	0.771	0.777
ST(1.0)	112					

used. The latter sample was prepared solvothermally in 2-methylaminoethanol.[10]

2.4. Analysis of the Species Adsorbed on the Catalysts. Temperature-programmed desorption (TPD) of the adsorbed species except for NH_3 was carried out in a fixed-bed flow reactor. The catalyst was heated at 650 °C for 30 min in He and cooled to 100 °C, and a gas with a prescribed composition was allowed to flow over the catalyst at $W/F = 0.3$ g·s·mL^{-1} for 1 h. After the excess adsorbate gas was purged with a He flow, the catalyst was heated to 700 °C at a rate of 5 °C·min^{-1} in a He flow, and the desorbed species were analyzed with the Q-Mass detector.

The NH_3 TPD measurement was carried out with a Bel-Japan TPD-1-AT analyzer. The powdered sample (0.4 g) was placed in the TPD cell and pretreated in a 50 mL·min^{-1} He flow at 500 °C for 1 h. Then, the sample was exposed to 2.7 kPa NH_3 at 100 °C for 10 min. After evacuation for 1 h, the sample was heated to 600 °C at a rate of 10 °C·min^{-1} in a He flow, and the effluent gases were analyzed with the Q-Mass detector.

A Nicolet Magna-IR system 560 FT-IR diffuse reflectance spectrometer (resolution: 4 cm^{-1}) was used to detect the adsorbed species on the catalyst surface. The sample was pretreated at 500 °C in a 30 mL·min^{-1} He flow for 1 h; then, the background spectrum was obtained. The spectra of the adsorbed species are given as difference spectra obtained by subtraction of the background.

3. Results and Discussion

3.1. Crystal Structures of the Catalysts. The XRD pattern of ST(0.0) indicates that the alumina synthesized by the solvothermal method in diethylenetriamine is amorphous (Figure S1 in the Supporting Information). The Ga_2O_3-containing mixed oxides exhibited the patterns due to the spinel structure, and their peaks shifted to the lower angle side with an increase in Ga content, indicating that substitution of Al^{3+} ions with larger Ga^{3+} ions resulted in an enlargement of the unit cell parameter. Therefore, all of the products except for ST(0.0) and ST(1.0) are solid solutions of γ-Ga_2O_3−Al_2O_3.

Upon calcination at 700 °C, a part of ST(1.0) was transformed into the β phase of Ga_2O_3, whereas ST(0.0) gave poorly crystallized Al_2O_3. The other mixed oxides preserved the γ-phase structure after calcination at 700 °C, although their crystallite sizes were slightly enlarged (Figure S2 in the Supporting Information).

The surface areas and chemical compositions of the catalysts (calcined samples) are summarized in Table 1. The surface area of the catalyst tends to decrease with the increase in the Ga content.

The ICP analysis showed that the catalysts with high Ga contents (e.g., ST(0.75) and ST(0.5)) had almost the same compositions as those of the starting materials for solvothermal synthesis, whereas for the catalysts with low Ga contents, Ga^{3+} ion contents in the products were smaller than those expected from the feed composition.

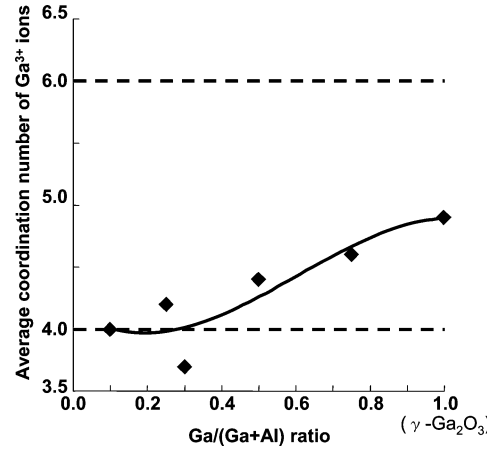

Figure 1. Average coordination numbers of Ga in the γ-Ga_2O_3−Al_2O_3 catalysts calculated from the EXAFS spectra of the catalysts: Fitting parameters are as follows: FT range, 3.3−14.0 Å^{-1}; FT k weight, 3; fitting space, R space; fitting R range, 1.0 to 1.8 Å; fitting k weight, 3.

The XPS analysis indicated that the catalysts with high Ga contents (ST(0.75) and ST(0.5)) had constant Ga concentrations from surface to bulk, whereas those with small Ga contents (ST(0.3) and ST(0.25)) had Ga-rich surface compositions, indicating the presence of a Ga concentration gradient inside the particles. Actually, ST(0.3) exhibited an obvious Ga concentration gradient; the Ga concentration decreased gradually at deeper points from the surface. Therefore, the Ga_2O_3−Al_2O_3 catalysts with small Ga contents had larger numbers of surface Ga sites than those expected from the bulk compositions.

Figure 1 shows the average coordination numbers of Ga^{3+} ions calculated from the EXAFS spectra. The normalized absorption data of XANES spectra are shown in Figure S3 in the Supporting Information. For the value at Ga/(Ga + Al) = 1.0, the datum for pure γ-Ga_2O_3 is plotted because ST(1.0) was composed of γ and β phases. The average coordination number of Ga^{3+} ion in pure γ-Ga_2O_3 was calculated to be 4.9, which is slightly smaller than the theoretical value. The average coordination number decreased with the decrease in the Ga content and converged at about 4 for the catalysts with low Ga contents. This indicates that Ga^{3+} ions predominantly occupy the tetrahedral sites; therefore, the γ-Ga_2O_3−Al_2O_3 binary oxides are not simple solid solutions. Nearly all of the Ga^{3+} ions in ST(0.3) are located in the tetrahedral sites, whereas Al^{3+} ions predominantly occupy the octahedral sites in the spinel structure. Similar results have been previously reported.[3,11,22] Spinels belong to the *Fd3m* space group. There are eight formula units per cubic unit cell. Anions are located in Wycoff 32e sites whose coordinates are (u, u, u). The anion sublattice of ideal spinel is in cubic closest-packed (ccp) arrangement. Because the coordinates of the anions at 32e sites are not special, they can vary according to a single parameter, u. For a perfect ccp anion arrangement, $u = 0.375$. As u increases from its ideal value, anions move away from the tetrahedrally coordinated A-site cations along the <111> directions toward the center of three B-site cations, which increases the volume of each A-site interstice. Therefore, the spinel structure can accommodate large cations in the tetrahedral sites.[23]

Because γ-Ga_2O_3−Al_2O_3 is made of two metal elements both with the same valence of 3+ (Ga^{3+} and Al^{3+}), cation vacancies

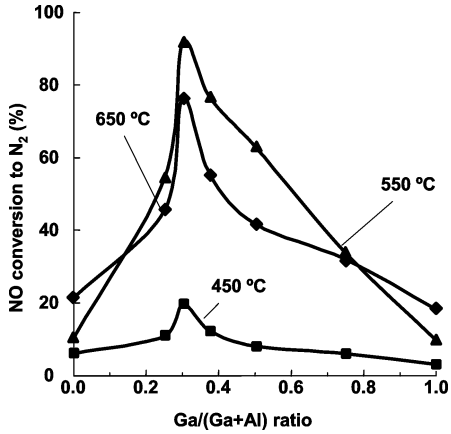

Figure 2. Effect of Ga/(Ga + Al) ratios of the γ-$Ga_2O_3-Al_2O_3$ catalysts on their NO conversion to N_2. Reaction conditions: 1000 ppm NO, 2000 ppm CH_4, 6.7% O_2, and 2.5% H_2O with He balance; SV = 11 000 h^{-1}.

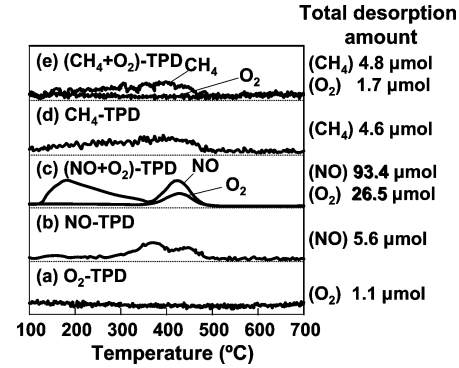

Figure 3. TPD profiles of (a) O_2, (b) NO, (c) NO−O_2, (d) CH_4, and (e) CH_4-O_2 adsorbed on ST(0.3) catalyst. The catalyst was pretreated in He at 650 °C for 30 min, and then the reactant gas diluted to a desired concentration with He was allowed to flow at 100 °C for 1 h. After the gas was purged with a He flow, desorption was carried out in a 100 mL·min^{-1} He flow at a heating rate of 5 °C·min^{-1}. Gases: 1000 ppm NO, 2000 ppm CH_4, and/or 6.7% O_2.

should be incorporated in the spinel structure because of charge imbalance. Therefore, one-ninth of the total cation sites available for the spinel structure are vacant ($M^{3+}{}_{8/3}\square_{1/3}O_4$, M^{3+}: Ga^{3+} or Al^{3+}). Here we will deal with γ-$Ga_2O_3-Al_2O_3$ with an extreme structure in which Ga^{3+} and Al^{3+} ions solely occupy tetrahedral and octahedral sites, respectively. When the cation vacancies exist only in the tetrahedral sites ($[Ga_{2/3}\square_{1/3}]^{tet}[Al_2]^{oct}O_4$), the Ga/(Ga + Al) ratio is calculated to be 0.25. When the vacancies exist solely in the octahedral sites ($[Ga_1]^{tet}[Al_{5/3}\square_{1/3}]^{oct}O_4$), the Ga/(Ga + Al) ratio would be 0.375. Therefore, the data for ST(0.3) shown in Figure 1 and Table 1 (coordination number of Ga is ca. 4 for Ga/(Ga + Al) ratio of around 0.25) indicate that the cation vacancies mainly exist in the tetrahedral sites of the spinel structure.

3.2. Catalytic Activity. Figure 2 shows the activity change of the catalysts for NO conversion to N_2 as a function of the Ga/(Ga + Al) ratio. Both ST(0.0) and ST(1.0) had very low activity, indicating that the combination of Ga and Al ions is a crucial factor for the catalytic activity. The conversion of NO to N_2 reached a maximum for ST(0.3) in which Ga^{3+} and Al^{3+} ions preferentially occupy the tetrahedral and octahedral sites, respectively. Each oxygen anion in the spinel (AB_2O_4) coordinates to one tetrahedral A cation and three octahedral B cations. Therefore, the catalyst that exhibited the highest activity has the largest number of tetrahedral Ga^{3+} ions with octahedral Al^{3+} ions at the next-nearest neighbor sites. When the Ga/(Ga+Al) ratio exceeds 0.3, the population of $Ga^{tet}-O-Ga^{oct}$ bonds increases.

3.3. Desorption of the Reactants Adsorbed on the Catalysts. Figure 3 shows the TPD profiles of the reactants adsorbed on ST(0.3) that showed the highest activity. When the catalyst was exposed to an NO/He flow (Figure 3b), two desorption peaks of NO were observed at about 350 and 450 °C, and the latter peak was associated with desorption of a trace amount of O_2. When NO and O_2 were coadsorbed on the catalyst, a much larger amount of NO was adsorbed, and the desorption peaks of NO were observed at around 200 and 400 °C. The latter peak was associated with a desorption peak of O_2 (Figure 3c) despite the fact that O_2 itself was not adsorbed on the catalyst (Figure 3a). These results indicate that O_2 had an ability to change the state of NO so as to be easily adsorbed on the catalyst surface. The amount of desorbed O_2 at 450 °C was about half of the amount of desorbed NO at the same temperature. Haneda et al.[4] reported similar NO−O_2 TPD profiles for $Ga_2O_3-Al_2O_3$ catalysts prepared by a sol−gel method and attributed the former and latter peaks to the surface nitrite and nitrate species, respectively. It is interesting to note that a large low-temperature peak was observed when NO and O_2 were coadsorbed. Because the formation of nitrite species from NO is an oxidation process, it is reasonable to assume that oxygen is required for the formation of surface nitrite species, and the following sequence was proposed for this process[24]

$$NO + {}^1/_2O_2 \rightarrow NO_2 \quad (2)$$

$$NO + NO_2 \rightarrow N_2O_3 \quad (3)$$

$$M-O-M + N_2O_3 \rightarrow 2MONO \quad (4)$$

Equation 4 may be rewritten as follows

$$2MOH + N_2O_3 \rightarrow 2MONO + H_2O \quad (5)$$

If these arguments are correct, then the desorption process of NO would be accompanied by the formation of O_2. This was not the case, as is shown in Figure 3c. Therefore, we temporarily attribute the desorption of NO to the formation of NO and surface nitrate species from the adsorbed NO_2 as shown in eq 6

$$3NO_2(ad) + 2MOH \rightarrow NO + 2MONO_2 + H_2O \quad (6)$$

This reaction is essentially identical to the formation of nitric acid by the reaction of NO_2 with water. However, this reaction would contribute to the SCR of NO by the formation of surface nitrate species and would not be directly connected with the SCR of NO because the desorption of NO takes place at a much lower temperature than the working temperature of the catalyst for SCR.

The amount of adsorbed CH_4 was quite small, as shown in Figure 3d. This result is due to the fact that a higher temperature is required for adsorption of methane, as will be discussed later. However, different phenomena were observed for ethylene or propylene TPD, where significant uptakes were observed even when the catalyst was exposed to these gases at 100 °C.[13,18] As

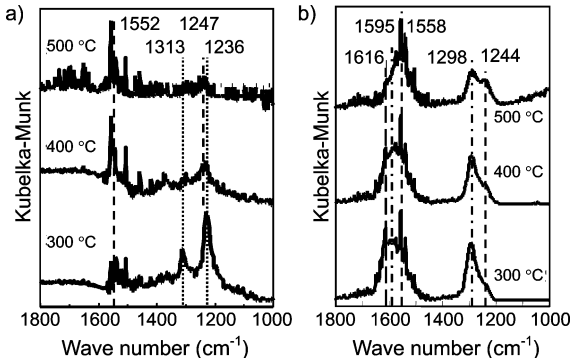

Figure 4. FT-IR spectra of the ST(0.3) treated with NO in the presence and absence of O_2. Adsorption was carried out with (a) 1000 ppm NO and (b) 1000 ppm NO−6.7% O_2, both with He balance at 100 °C for 90 min. Then, the catalyst was heated in situ in a He flow at the desired temperature specified in the Figure.

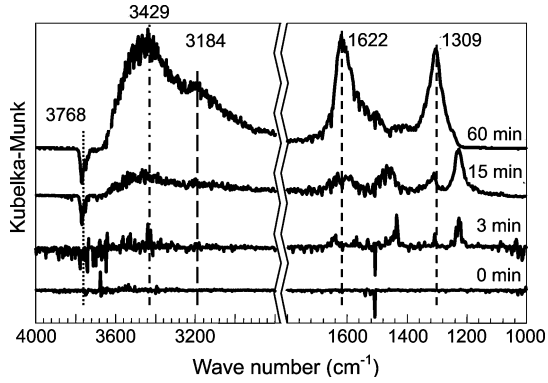

Figure 5. Time course change in the FT-IR spectra of NO species adsorbed on ST(0.3) in the presence of O_2. ST(0.3) was exposed to 1000 ppm NO and 6.7% O_2 with He balance at 100 °C.

shown in Figure 3e, CH_4 uptake did not change, even in the presence O_2.

The adsorbed state of NO was investigated by FT-IR spectroscopy (Figure 4). When NO was introduced in the absence of O_2, an intense band developed at 1236 cm^{-1} together with less intense bands at 1313 and around 1550 cm^{-1}. Most researchers assign the peak at 1230 cm^{-1} to a bridging nitrite species.[25,26] These bands decreased in intensity with an increase in the temperature and almost disappeared at 500 °C. These results are in good agreement with the TPD results; however, small absorption bands that can be attributed to nitrate species were still observed at 500 °C.

Different spectra were observed when NO was fed in the presence of O_2; five bands appeared at 1244, 1298, ∼1560, ∼1600, and ∼1620 cm^{-1} at 300 °C. Because the wave numbers are essentially identical to those of the bands observed when NO_2 was adsorbed on alumina,[27] all of the observed bands can be assigned to nitrate species. The intensities of the bands decreased as the temperature increased, and species that exhibit bands at 1244 and ∼1560 cm^{-1} remained after heat treatment at 500 °C. Although the assignment of the bands of surface nitrate species is a controversial issue,[15,17] we temporarily assigned these two bands to asymmetric and symmetric vibration modes of bridging bidentate nitrate species because this species is the most stable among the possible structures of surface nitrate species.[26]

Figure 5 shows the time-course change in the FT-IR spectra of surface species formed on ST(0.3) by exposure to an NO−O_2−He flow at 100 °C. Nitrite species were formed first, which were converted to other species after 1 h of exposure.

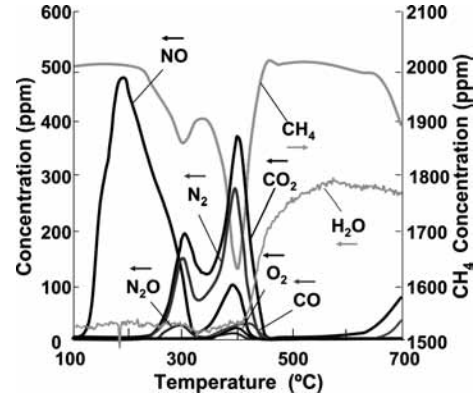

Figure 6. Reaction of CH_4 with NO adsorbed on ST(0.3) in the presence of O_2. ST (0.3) was exposed to 1000 ppm NO−6.7% O_2 with He balance at 100 °C for 1 h, purged with a He flow, and then heated at a rate of 5 °C·min^{-1} in a 100 mL·min^{-1} flow of 2000 ppm CH_4/He.

The IR spectrum of this surface species resembled that of the surface nitrate species (Figure 4b); however, peaks are observed at higher wave numbers. Therefore, predominant species was assigned as adsorbed NO_2 strongly interacting with the surface hydroxyl groups. Although we believe that a part of the adsorbed NO_2 was converted into surface nitrate species in this stage, complete conversion into surface nitrate species can be ruled out because of the formation of NO in the NO−O_2 TPD profile because the condition adopted for obtaining the top spectrum in Figure 5 (i.e., exposure to a gas composed of 1000 ppm NO and 6.7% O_2 with helium balance at 100 °C for 1 h) is essentially identical to the adsorption conditions for the TPD experiment. These results show a sharp contrast with the result reported by Haneda et al.,[4] who described that nitrite species are predominant when their Ga_2O_3−Al_2O_3 catalyst is exposed to NO−O_2 at temperatures below 473 K. As surface nitrate species developed, a negative band appeared at 3768 cm^{-1}, and simultaneously, a broadband at 3600−3000 cm^{-1} grew. The former band is assigned to the isolated hydroxyl group[29,30] and the latter band is assigned to adsorbed water.[31] The formation of adsorbed water can be explained by eq 6 or by the following reaction

$$2NO + 3/2O_2 + 2M{-}OH \rightarrow 2M{-}O{-}NO_2 + H_2O \quad (7)$$

3.4. Reaction between Methane and Surface Species Derived from NO−O_2. The reaction between methane and surface species derived from NO−O_2 was investigated. After ST(0.3) was treated with NO in the presence of O_2 at 100 °C, CH_4/He was introduced on the catalyst, and the composition of the effluent gas was analyzed by the Q-Mass detector (Figure 6). Similar to the NO−O_2 TPD profile (Figure 3c), desorption of NO was observed at around 200 °C, indicating that a higher temperature is required to proceed the reaction of CH_4 with adsorbed NO_2. However, the concentration of NO in the effluent gas drastically decreased above 250 °C with a concomitant decrease in CH_4, suggesting that adsorbed NO_2 was reduced with CH_4. In the temperature range from 250 to 450 °C, N_2, N_2O, CO_2, and CO were formed, each giving two peaks at low and high temperatures. The lower-temperature peaks may be due to the reaction of methane with adsorbed NO_2, whereas higher-temperature peaks can be attributed to the reaction of methane with surface nitrate species. These results show a sharp contrast with the results reported by He et al.,[15] who showed

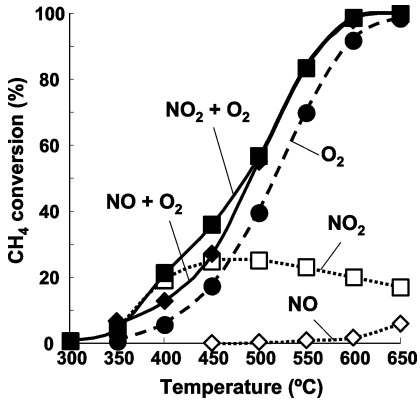

Figure 7. Reaction of methane with various oxidants on ST(0.3). Reaction conditions: 2000 ppm CH_4, 1000 ppm NO or NO_2, and 2.5% H_2O with/without 6.7% O_2 balanced with He; SV = 11 000 h^{-1}.

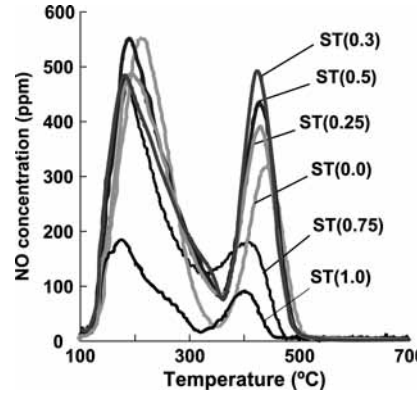

Figure 8. TPD profiles of NO on γ-Ga_2O_3−Al_2O_3 catalysts. The catalysts were pretreated in a He flow at 650 °C for 30 min and exposed to the gas mixture (1000 ppm NO and 6.7% O_2 with He balance) at 100 °C for 1 h. After NO was purged with a He flow, the desorption was carried out in the He flow (100 mL·min^{-1}) at a heating rate of 5 °C·min^{-1}.

that IR spectra of the surface nitrate species adsorbed on their Ga_2O_3/Al_2O_3 catalyst were not changed after exposure to C_3H_8 at 300 °C. From the results, they concluded that those surface nitrate species are "spectators" and are not involved in the SCR reaction. However, the present results clearly showed that surface nitrate species do react with methane in the temperature range where the catalyst showed high activity for methane-SCR of NO.

The same result was obtained when ST(0.3) impregnated with a small amount of $Al(NO_3)_3$ or $Ga(NO_3)_3$ was heated in a CH_4/He flow (data not shown). However, low-temperature desorption of NO without the formation of O_2 was not observed. When NO was adsorbed in the absence of O_2, the formation of N_2 was scarcely observed because NO has only low oxidizing ability. Therefore, surface nitrate species play a crucial role in methane-SCR of NO in the presence of O_2.

Figure 7 shows methane oxidation with various oxidants on ST(0.3). Whereas NO had essentially no reactivity, even at 600 °C, methane was oxidized by NO_2 at a temperature as low as 350 °C, even in the absence of O_2. Although the concentration of NO_2 fed to the reactor was much lower than that of O_2, the amount of methane oxidized by NO_2 at 350 °C was much larger than that oxidized by O_2, indicating that the oxidation ability of NO_2 was superior to that of O_2. Therefore, NO_2 is highly reactive for the oxidation of CH_4. At higher temperatures, however, the methane conversion by NO_2 rather decreased, probably because of its decomposition to NO and O_2 (eq 8)

$$2NO_2 \rightarrow 2NO + O_2 \quad (8)$$

This reaction can occur either in the gas phase or on the catalyst, and the gas-phase reaction is well established because the reverse reaction of eq 8 is an important reaction for the synthesis of nitric acid.[28] To verify the catalytic activity for reaction eq 8, we examined NO_2 decomposition on the catalyst (Figure S4 in the Supporting Information); the result clearly shows that the present catalyst significantly facilitates the reaction. Therefore, the decrease in CH_4 conversion at high temperatures is caused by the decomposition of NO_2 on the catalyst. From the microscopic reversibility, the catalyst should also facilitate the reverse reaction of eq 8, which is an important process for the formation of surface nitrate species from NO and O_2. As discussed earlier, surface nitrate species, which can be formed by exposure of the catalyst to either NO + O_2 or NO_2, decompose into NO and O_2 at higher temperatures; therefore, decomposition of NO_2 can take place via decomposition of surface nitrate species. This argument is supported by the fact that both of the reactions (NO_2 decomposition and decomposition of surface nitrate species yielding NO and O_2) started at the same temperature (~375 °C).

In the presence of O_2, both NO and NO_2 exhibited high reactivity for the oxidation of methane in the whole temperature range. This fact again shows the importance of oxygen in methane-SCR of NO in the temperature range of 350−500 °C. In this temperature range, $NO_2 + O_2$ was slightly more reactive toward methane than $NO + O_2$, indicating that the participation of NO_2 is important at lower temperatures.

3.5. Sites for the Formation of Surface Nitrate Species. Because the peak at around 450 °C in the NO−O_2 TPD profiles is due to surface nitrate species, the number of surface sites giving these species can be estimated from the intensity of this peak. Figure 8 shows the NO−O_2 TPD profiles of the γ-Ga_2O_3−Al_2O_3 catalysts with various Ga/Al ratios. The largest peak was observed for ST(0.3), indicating that this catalyst had the largest number of the sites for the formation of surface nitrate species. The order of the peak intensity, ST(0.3) > ST(0.5) > ST(0.25) > ST(0.0) > ST(0.75) > ST(1.0), was in good agreement with the order of catalytic activity (Figure 2), indicating that the sites for the formation of surface nitrate species play an important role in the methane-SCR of NO. Similar results were reported by Haneda et al.[4] for the Ga_2O_3−Al_2O_3 catalyst prepared by a sol−gel method. However, the optimal composition is different between theirs and ours presumably because of the difference in the catalyst synthesis processes.

As the Al content in the catalyst increased, the desorption peak shifted to the higher temperature side, indicating that Al interacts more strongly with surface nitrate species than Ga. Moreover, the amounts of NO desorbed from the Ga-rich catalysts were remarkably smaller than those from the other catalysts. This result as well as the lower desorption temperature suggests that surface nitrate species anchored on the Ga sites have a character that is significantly different from those of the nitrate species anchored on the Al sites.

Because the formation of surface nitrate species is accompanied by consumption of the isolated hydroxyl groups, the FT-IR spectra in the OH stretching vibration region of the catalysts with various Ga contents were examined after exposure to NO−O_2 (Figure S5 in the Supporting Information). Although the spectra are not well resolved, two negative bands are

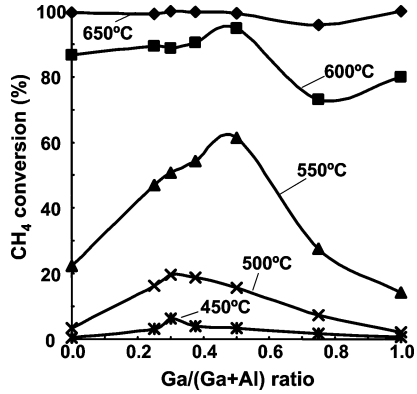

Figure 9. CH_4 conversion in methane-SCR of NO on the γ-Ga_2O_3−Al_2O_3 catalysts. Reaction conditions are shown in the caption of Figure 2.

apparently observed at 3768 and 3686 cm^{-1}. The band at 3768 cm^{-1} was observed for the Al-rich catalysts but not for the Ga-rich catalysts. On the contrary, the 3686 cm^{-1} band was observed for the Ga-rich catalyst but not for the Al-rich catalyst. Therefore, the former band was assigned to isolated Al−OH and the latter band was assigned to isolated Ga−OH.[15,30]

3.6. Base Property of Isolated Hydroxyl Group. The basicity of the catalysts was investigated by CO_2-TPD (Figure S6 in the Supporting Information). Pure Ga_2O_3 adsorbed only a small amount of CO_2, and the CO_2 uptake corresponding to the number of base sites increased monotonically with the increase in Al content in the catalyst (Figure S6 in the Supporting Information).

The FT-IR spectra of CO_2 species adsorbed on the catalysts with various Ga contents exhibited bands due to hydrogen carbonate species together with a negative band due to isolated Al−OH for the catalysts containing Al (Figure S7 in the Supporting Information). Hydrogen carbonate is supposed to be formed when the hydroxyl group with a basic nature interacts with CO_2.[32] For pure Ga_2O_3, no negative band due to isolated GaOH was observed (Figure S7 in the Supporting Information) because of low CO_2 uptake on this catalyst (Figure S6 in the Supporting Information). Because both the nitrate and hydrogen carbonate species seem to be formed on the same Al−OH sites, the basicity of the group plays an important role in the formation of surface nitrate species. However, basicity is not the sole factor because the maximum amount of surface nitrate species was formed on ST(0.3) despite the fact that the maximum CO_2 uptake was observed for ST(0.0); the combination between base sites and Ga sites seems to be important.

3.7. Activation of Methane. Figure 9 depicts the conversion of methane in methane-SCR of NO shown in Figure 2. At 550 and 600 °C, the highest methane conversion was observed on ST(0.5), whereas ST(0.3) exhibited the highest methane conversion at 450 and 500 °C. In the previous work,[10] we examined the correlation between the performance for methane-SCR and the acidity of the catalysts prepared solvothermally in various media and found that the surface acid density of the catalyst is predominantly determined by the reaction medium used for the catalyst synthesis. Diethylenetriamine adopted in this work gives the catalyst with the smallest surface acid density. We also found that the combustion of methane occurs competitively with methane-SCR of NO, especially at high temperatures, and that a higher acid density facilitates the combustion of methane, thus leading to lower efficiency of methane used for SCR.[10]

$$CH_4 + 2O_2 \rightarrow CO_2 + 2H_2O \quad (9)$$

Therefore, the acidity of the catalysts used in this work was assessed by the NH_3-TPD method (data not shown). For the catalysts with low Ga contents, the acid density monotonically increased with the increase in the Ga content, and ST(0.5) had the largest number of acid sites. This result explains the reason why ST(0.5) exhibited the highest methane conversions at higher temperatures, as shown in Figure 9.

Lewis acid properties of Ga_2O_3−Al_2O_3 catalysts as well as Al_2O_3 and Ga_2O_3 have been well documented.[22,32−34] These Lewis acid properties originate from coordinatively unsaturated ions and tetrahedral Ga^{3+} ions emerging at the extended crystal surface.[32−34]

The acid strength was assessed by the desorption temperature of NH_3. ST(0.3) exhibited the highest acid strength (peak temperature at which the maximum rate for desorption of NH_3 was observed was 255 °C). The high performance of this catalyst for methane-SCR can be explained by the fact that these highly acidic sites are effective for methane activation relating to methane-SCR of NO. When pure γ-Ga_2O_3 and γ-Al_2O_3 are compared (peak temperatures were 237 and 207 °C, respectively), γ-Ga_2O_3 has higher acid strength. However, the acid strengths of the mixed oxides were higher than those of the single-component catalysts, indicating that the synergistic effect of Ga and Al determines the acid nature of the catalysts.

To examine the interaction of methane with the catalysts, 2000 ppm CH_4 in He was fed on the catalysts with increasing reaction temperature of 5 °C·min^{-1} (Figure 10). The methane concentration first decreased (at ∼200 °C) and then increased (at ∼400 °C), indicating that adsorption and desorption of methane took place at these temperatures. The relatively high adsorption temperature suggests that activation energy is required for methane to be adsorbed on the catalyst. The largest methane uptake was observed for ST(0.5) that has the largest number of acid sites. It must be noted that methane was not adsorbed on ST(0.0) at all, indicating that the adsorption of methane takes place on the Ga sites rather than on the Al sites.

The decrease in methane concentration was also observed at above 600 °C, and CO and H_2 were formed at these temperatures (Figure S8 in the Supporting Information). This result indicates that the reduction of the catalyst occurred. However, ST(0.0) showed neither consumption of methane (Figure 10) nor CO formation (Figure S8 in the Supporting Information), indicating that Al_2O_3 does not have a redox property. The consumption of methane at 700 °C increased with the increase in Ga content in the catalyst, and accordingly, the formation of CO increased. Therefore, Ga_2O_3 does have a redox property, but Al_2O_3 does not.

Although Al_2O_3 is reduced to Al_2O or $AlO·Al_2O_3$ by treatment with Al metal at high temperature,[35] the reduction of Al_2O_3 cannot occur under the present reaction conditions because the reduction potential of Al^{3+} is highly negative. However, Ga^{3+} has a less-negative reduction potential, and Ga_2O_3 can be reduced to gallium oxides with lower oxidation states under conditions similar to the present one.[36] He et al.[15] discussed the reaction mechanism of propane-SCR of NO on the assumption that neither Ga_2O_3 nor Al_2O_3 are redox-active materials. However, Ga_2O_3 has a redox property. This property seems to be important not only for the activation of methane but also for the oxidation of NO to surface nitrate species. The smaller amount of surface nitrate species formed on the catalysts with high Al contents may be due to the lack of this redox property despite the fact that they had much larger numbers of base sites.

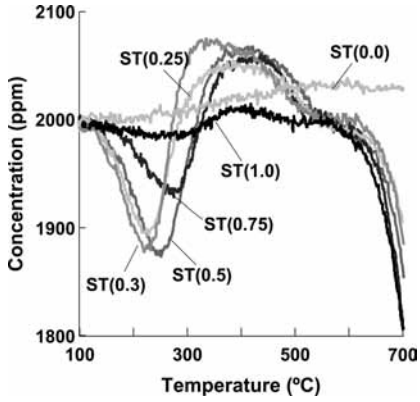

Figure 10. Temperature-programmed reaction of CH_4 with the γ-$Ga_2O_3-Al_2O_3$ catalysts. The catalysts (0.5 g) were heated in a 100 $mL \cdot min^{-1}$ flow (SV = 11 000 h^{-1}) of 2000 ppm CH_4/He at a heating rate of 5 $°C \cdot min^{-1}$.

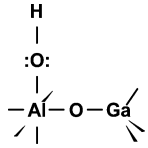

Figure 11. Proposed active site of the γ-$Ga_2O_3-Al_2O_3$ catalyst for methane-SCR of NO.

3.8. Active Site of the Catalyst for Methane-SCR of NO. The active site of the catalyst for methane-SCR of NO was proposed as depicted in Figure 11. First, NO is adsorbed on the isolated hydroxyl group bonded to Al that acts as a base site. Then, the adsorbed NO is oxidized to surface nitrate species by O_2; here the presence of Ga with a redox property is quite important. However, methane is activated on the tetrahedral Ga site (coordinatively unsaturated site); this site acts not only as a Lewis acid site but also as a redox site. The most important factor is the presence of the surface nitrate species formed on the Al sites neighboring the tetrahedral Ga sites that activate methane. When the site for the formation of surface nitrate species is not present near the methane activation site, the activated methane will react with only O_2 in the gas phase (combustion). Although ST(0.5) has a larger number of acid sites (that is, methane activation sites), the number of Ga−Al ensembles suitable for the cooperation is small compared with ST(0.3). Therefore, ST(0.3) has higher performance than ST(0.5) despite the fact that the higher methane conversion was observed on the latter catalyst.

4. Conclusions

The γ-$Ga_2O_3-Al_2O_3$ catalysts prepared by the solvothermal reaction of gallium acetylacetonate and aluminum isopropoxide in diethylenetriamine had a spinel structure in which Ga^{3+} and Al^{3+} ions tend to occupy the tetrahedral and octahedral sites, respectively. When the Ga/(Ga+Al) ratio was 0.3, almost all tetrahedral sites and octahedral sites were occupied by Ga^{3+} and Al^{3+} ions, respectively, and the catalyst exhibited the highest performance for methane-SCR of NO. The active site was deduced to be related to the combination of the tetrahedral Ga^{3+} ion with octahedral Al^{3+} ions in the next-nearest-neighbor sites. The following reaction mechanism was proposed: On one hand, NO is adsorbed on the isolated hydroxyl groups on Al ions that act as the base sites and then oxidized to the surface nitrate species by O_2. On the other hand, methane is activated on Lewis acid sites that are supposed to originate from tetrahedral Ga ions. In addition, the γ-$Ga_2O_3-Al_2O_3$ catalyst has a redox property developed by Ga ions. This redox property is important for both the oxidation of NO to surface nitrate species and the activation of methane. The most important factor of this catalyst is the presence of the site for the formation of surface nitrate species (octahedral Al) near the methane activation site (tetrahedral Ga). Therefore, the ST(0.3) that has the highest number of Ga−Al ensembles exhibited the highest performance for methane-SCR of NO.

Acknowledgment. This work was partially supported by a Grant-in-Aid for Scientific Research from the Ministry of Education, Culture, Sports, Science and Technology, Japan. We are grateful to Prof. S. Imamura for his kind help and discussions. The XAFS experiments were performed at BL16B2 in SPring-8 with the approval of the Japan Synchrotron Radiation Research Institute (JASRI) (proposal no. C05A16B2-4050-N).

Supporting Information Available: XRD patterns, XAFS spectra, decomposition of NO_2, FT-IR spectra, TPD profiles, and formation of CO. This material is available free of charge via the Internet at http://pubs.acs.org.

References and Notes

(1) (a) Iwamoto, M.; Yahiro, H. *Catal. Today* **1994**, *22*, 5. (b) Armor, J. N. *Catal. Today* **1995**, *26*, 147. (c) Li, Y.; Armor, J. N. *J. Catal.* **1995**, *145*, 1.

(2) Shimizu, K.; Satsuma, A.; Hattori, T. *Appl. Catal., B* **1998**, *16*, 319.

(3) Shimizu, K.; Takamatsu, M.; Nishi, K.; Yoshida, H.; Satsuma, A.; Tanaka, T.; Yoshida, S.; Hattori, T. *J. Phys. Chem. B* **1999**, *103*, 1542.

(4) Haneda, M.; Kintaichi, Y.; Mizushima, T.; Kakuta, N.; Hamada, H. *Appl. Catal., B* **2001**, *31*, 81.

(5) (a) Lezcano, M.; Ribotta, A.; Miro, E.; Lombardo, E.; Petunchi, J.; Moreaux, C.; Dereppe, J. M. *J. Catal.* **1997**, *168*, 511. (b) Sowade, T.; Schütze, F.-W.; Berndt, H.; Grünert, W. *Chem. Eng. Technol.* **2004**, *27*, 1277.

(6) Schulz, P.; Baerns, M. *Appl. Catal.* **1991**, *78*, 15.

(7) Tabata, T.; Kokitsu, M.; Okada, O. *Appl. Catal., B* **1995**, *6*, 225.

(8) (a) Inoue, M.; Kominami, H.; Inui, T. *J. Chem. Soc., Dalton Trans.* **1991**, 3331. (b) Inoue, M. *J. Phys.: Condens. Matter* **2004**, *16*, S1291. (c) Iwamoto, S.; Inoue, M. *J. Jpn. Pet. Inst.* **2008**, *51*, 143.

(9) (a) Inoue, M.; Inoue, N.; Yasuda, T.; Takeguchi, T.; Iwamoto, S. *Adv. Sci. Technol.* **2000**, *29*, 1421. (b) Takahashi, M.; Inoue, N.; Nakatani, T.; Takeguchi, T.; Iwamoto, S.; watanabe, T.; Inoue, M. *Appl. Catal., B* **2006**, *65*, 142.

(10) Takahashi, M.; Nakatani, T.; Iwamoto, S.; Watanabe, T.; Inoue, M. *Appl. Catal., B* **2007**, *70*, 73.

(11) Takahashi, M.; Inoue, N.; Takeguchi, T.; Iwamoto, S.; Watanabe, T.; Inoue, M. *J. Am. Ceram. Soc.* **2006**, *89*, 2158.

(12) (a) Takahashi, M.; Nakatani, T.; Iwamoto, S.; Watanabe, T.; Inoue, M. *Ind. Eng. Chem. Res.* **2006**, *45*, 3678. (b) Takahashi, M.; Nakatani, T.; Iwamoto, S.; Watanabe, T.; Inoue, M. *J. Phys.: Condens. Matter* **2006**, *18*, 5745.

(13) Miyahara, Y.; Takahashi, M.; Masuda, T.; Imamura, S.; Kanai, H.; Iwamoto, S.; Watanabe, T.; Inoue, M. *Appl. Catal., B* **2008**, *84*, 289.

(14) Shimizu, K.; Satsuma, A.; Hattori, T. *Catal. Surv. Jpn.* **2000**, *4*, 115.

(15) He, C.; Paulus, M.; Find, J.; Nickl, J. A.; Eberle, H.; Spengler, J.; Chu, W.; Köhler, K. *J. Phys. Chem. B* **2005**, *109*, 15906.

(16) Haneda, M.; Joubert, E.; Ménézo, J.; Duprez, D.; Barbier, J.; Bion, N.; Daturi, M.; Saussey, J.; Lavalley, J.; Hamada, H. *J. Mol. Catal. A: Chem.* **2001**, *175*, 179.

(17) Haneda, M.; Bion, N.; Daturi, M.; Saussey, J.; Lavalley, J.; Duprez, D.; Hamada, H. *J. Catal.* **2002**, *206*, 114.

(18) Miyahara, Y.; Watanabe, T.; Masuda, T.; Kanai, H.; Deguchi, H.; Inoue, M. *J. Catal.* **2008**, *259*, 36.

(19) Sault, A. G.; Madix, R. J. *J. Phys. Chem.* **1986**, *90*, 4723.

(20) Moulder, F.; Stickle, W. F.; Sobol, P. E.; Bomben, K. D. *Handbook of X-ray Photoelectron Specrtroscopy*; Perkin-Elmer Co.: Eden Prairie, MN, 1992.

(21) Ravel, B.; Newville, M. *J. Synchrotron Radiat.* **2005**, *12*, 537.

(22) Otero Areán, C.; Rodríguez Delgado, M.; Montouillout, V.; Massiot, D. *Z. Anorg. Allg. Chem.* **2005**, *631*, 2121.

(23) Sickafus, K. E.; Wills, J. M.; Grimes, N. M. *J. Am. Ceram. Soc.* **1999**, *82*, 3279.

(24) Huang, H. Y.; Yang, R. T. *Langmuir* **2001**, *17*, 4997.
(25) (a) Centi, G.; Perathoner, S.; Biglino, D.; Giamello, E. *J. Catal.* **1995**, *151*, 75. (b) Sazama, P.; Čapek, L.; Drobná, H.; Sobalík, Z.; Dědeček, J.; Arve, K.; Wichterlová, B. *J. Catal.* **2005**, *232*, 302.
(26) Hadjiivanov, K. I. *Catal. Rev.−Sci. Eng.* **2000**, *42*, 71.
(27) Anderson, J. A.; Millar, G. J.; Rochester, C. H. *J. Chem. Soc., Faraday Trans.* **1990**, *86*, 571.
(28) Tsukahara, H.; Ishida, T.; Mayumi, M. *Nitric Oxide* **1991**, *3*, 191.
(29) Busca, G.; Lorenzelli, V.; Ramis, G.; Willey, R. J. *Langmuir* **1993**, *9*, 1492.
(30) Otero Areán, C.; Bellan, A. L.; Mentruit, M. P.; Rodríguez Delgado, M.; Palomino, G. T. *Microporous Mesoporous Mater.* **2000**, *40*, 35.
(31) Nortier, P.; Fourre, P.; Saad, A.; Saur, O.; Lavalley, J. C. *Appl. Catal.* **1990**, *61*, 141.
(32) Vimont, A.; Lavalley, J. C.; Sahibed-Dine, A.; Otero Areán, C.; Rodríguez Delgado, M.; Daturi, M. R. *J. Phys. Chem. B* **2005**, *109*, 9656.
(33) (a) Rodríguez Delgado, M.; Morterra, C.; Cerrato, G.; Magnacca, G.; Otero Aceán, C. *Langmuir* **2002**, *18*, 10255. (b) Lavalley, J. C.; Daturi, M.; Montouillout, V.; Clet, G.; Otero Areán, C.; Rodríguez Delgado, M.; Sahibed-dine, A. *Phys. Chem. Chem. Phys.* **2003**, *5*, 1301.
(34) Pushkar, Y. N.; Sinitsky, A.; Parenago, O. O.; Kharlanov, A. N.; Lunina, E. V. *Appl. Surf. Sci.* **2000**, *167*, 69.
(35) Hoch, M.; Johnston, H. L. *J. Am. Chem. Soc.* **1954**, *76*, 2560.
(36) (a) Biscardi, J. A.; Iglesia, E. *Catal. Today* **1996**, *31*, 207. (b) Meitzner, G. D.; Iglesia, E.; Baumgartner, J. E.; Huang, E. S. *J. Catal.* **1993**, *140*, 209.

JP901569S